https://doi.org/10.5194/egusphere-2024-3850
Preprint. Discussion started: 17 January 2025

A new method for large scale snow depth estimates using Sentinel-1 and ICESat-2

Rasmus Meyer[1], Mathias Preisler Schødt[1], Mikkel Lydholm Rasmussen[2], Jonas Kvist Andersen[1], Mads Dømgaard[1], Anders. Anker Bjørk[1].

[1]Department of Geosciences and Natural Resource Management, University of Copenhagen, Copenhagen Denmark
[2]DHI A/S, Hørsholm, 2970, Denmark

Correspondence: Rasmus Meyer (rpm@ign.ku.dk)

Abstract: Knowledge about seasonal snow accumulation is important for managing water resources, but accurate estimates of snow depth at a high spatiotemporal resolution are sparse, especially in mountainous regions. In this paper, we outline a novel approach to estimate snow depths using Sentinel-1 C-band synthetic aperture radar (SAR) and ICESat-2 LiDAR observations. Specifically, we estimate snow depths at 500-meter spatial resolution by correlating increase in Sentinel-1 volume scattering with snow depths derived using ICESat-2. Sentinel-1's vast spatial coverage and frequent 6/12-day revisit cycle makes it promising for monitoring seasonal snow accumulation, but capturing the volume scattering signal within a dry snowpack and relating it to snow depth remains challenging. Using ICESat-2, we retrieve thousands of high accuracy snow depth observations covering the Southern Norwegian Mountains. ICESat-2 has a low revisit time of three months, but by matching observations with the temporally nearest Sentinel-1 scene, we significantly enhance spatiotemporal resolution. Our results demonstrate that our ICESat-2 calibrated Sentinel-1 snow depths can estimate snowfall magnitudes in deep dry snow (>0.6 meters), achieving an accuracy of 0.5-0.7 meters, significantly improving estimates made by the SeNorge snow model in remote mountainous regions. This study highlights the potential of utilizing ICESat-2 to derive Sentinel-1 snow depths, improving snow monitoring capabilities in data-sparse regions.

1 Introduction

Snow is an important factor in the hydrological cycle in mountainous regions across the world. In these areas, precipitation is often stored in snowpacks, effectively creating a delay before water is discharged as meltwater with large interannual variation in magnitude. As temperatures rise globally, the seasonal timing of snowmelt changes (Adam et al., 2009). Snowmelt contributes the majority of water resources in many mountainous areas. For instance, it sustains 17% of the world's population with drinking water (Bormann et al., 2018), supplies communities with water for irrigation (Qin et al., 2020) and plays a crucial role in hydropower generation (Magnusson et al., 2020). Generally, snow is quantified by its snow water equivalent (SWE) through information about snow depth and snow density (Harder et al., 2016). Due to the depth of snow varying more than its density, much of the spatial variability of SWE can be described by the spatial variability of snow depth (López-Moreno et al., 2013). As such, knowledge about the depth of snow and its spatial distribution is key for calculating the amount of snowmelt runoff that a watershed can expect. However, measurements of total snow volume stored in mountainous areas are difficult to acquire as these places are often remote and vast, with rough terrain and harsh weather conditions. As such, current snow depth models rely on either numerical weather predictions, which lack

https://doi.org/10.5194/egusphere-2024-3850
Preprint. Discussion started: 17 January 2025

accurate snowfall information in mountainous areas, or interpolation between sparse in situ measurement stations(Saloranta, 2012; Kongoli et al., 2019)

Accurate snow depth estimations from remotely sensed laser altimetry (LiDAR) measurements are well documented (Deems et al., 2013; Nolan et al., 2015; Skaugen and Melvold, 2019). Airborne LiDAR campaigns can measure surface heights at centimeter precision, but cost and weather conditions limit the viability of this approach for regular snow depth estimates. The NASA Ice, Cloud and Land Elevation Satellite-2 (ICESat-2) was launched in 2018 and has since provided global laser altimetry measurements. Treichler and Kääb (2017) tested the utility of the first ICESat mission (operating from 2003 to 2010) when used for snow depth measurements in southern Norway. They proved that the vertical accuracy of ICESat showed promising results for snow depth estimation with a snow-off DEM available, but also noted the significant temporal and spatial limitations of ICESat. ICESat-2 has similar limitations, as the satellite scans the surface in track-lines with a temporal resolution of around three months, meaning that ICESat-2 snow depths alone cannot provide adequate information for studying seasonal changes in snow depths.

To achieve full spatial coverage, several studies have used radar polarimetry to measure snow depth or SWE showing a positive correlation between snow depth/SWE and increased volume scattering within a dry snowpack (Kendra et al., 1998; Lievens et al., 2019; Rott et al., 2010; Ulaby et al., 1984). Most studies researching the interaction between radar and snow have focused on the Ku- and X-bands as these frequencies are more sensitive to SWE changes and can be used in shallow snow (Du et al., 2010; King et al., 2015; Lievens et al., 2019; Rott et al., 2010). As C-band waves have a longer wavelength, and thus larger penetration depth, the received backscatter is predominantly influenced by soil properties from the ground surface under shallow snow (Pivot, 2012; Shi and Dozier, 2000). As a result, C-band Synthetic Aperture Radar (SAR) measurements have mostly been used for the detection of wet-snow (Longepe et al., 2009; Rott et al., 2010). However, the results of Lievens et al., (2019) suggest that C-band SAR can be used to estimate snow depths in deeper snow, where a gradual increase in backscatter is observed with the accumulation of dry snow. Lievens et al., (2022) applied C-band SAR from the Sentinel-1 satellites to create weekly snow depth maps in a sub-kilometer resolution over the European Alps, with the best results obtained in areas with snow depths between 1.5 m and 3 m.

In the present study, we combine open access satellite data from ICESat-2 and Sentinel-1 (Figure 1a-b) to estimate snow depths at 500 m spatial resolution over the open alpine regions of the Southern Norwegian Mountains. Our Sentinel-1 methodology is based on the change in cross-polarized ratio (ΔCR) as described in Lievens et al., (2019, 2022). ICESat-2 derived snow depths are used to calibrate the orbit-specific correlation between an increase in ΔCR and snow depths. Data is retrieved in the years 2019-2022 in snow accumulation months from January to April (Figure 1c). Results are compared on multiple scales; locally against snow depths measured at 12 alpine weather stations (Meteorologisk Institutt, 2024) and 279 in-situ measurements collected during a field excursion around Hardangervidda plateau from February 21 to 25, 2022. On a sub-regional scale with two ICESat-2 tracks covering a one of the most remote mountainous regions, in western Hardangervidda, and on a local to regional scale we compare our results with the numerical snow model “SeNorge” (NVE, 2024).

https://doi.org/10.5194/egusphere-2024-3850
Preprint. Discussion started: 17 January 2025

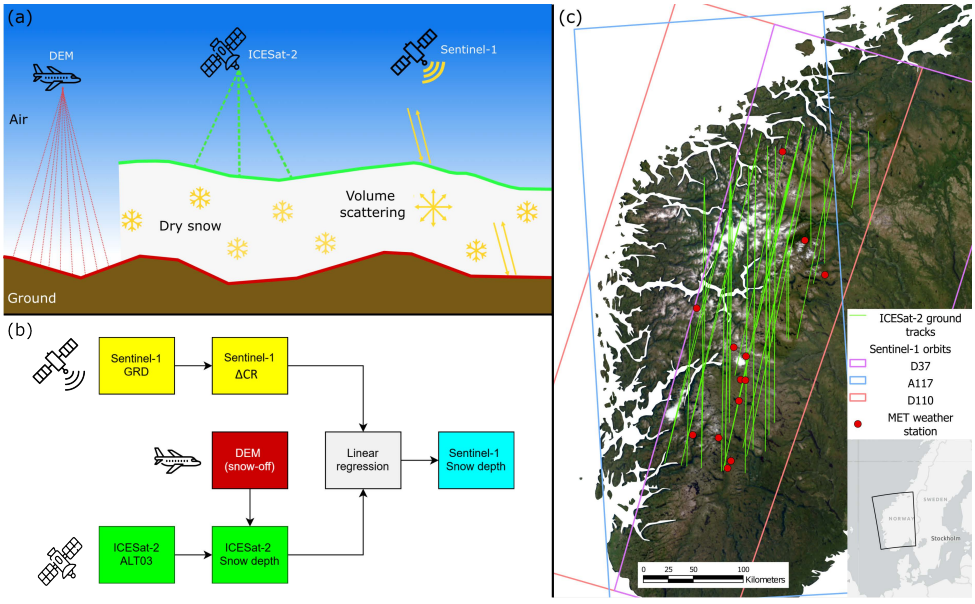

Figure 1: Concept and data inputs. (a) (b) ICESat-2 snow depths are derived based on the difference in height between the snow-on ICESat-2 surface height and a snow-off DEM. Sentinel-1 is used to extract the variable ΔCR, a proxy for change in volume scatting within a dry snowpack. Through linear regression between ICESat-2 and Sentinel-1, we retrieve continuous weekly snow depths in regions with little to no prior knowledge of snow depth. **(c)** Sentinel-1 orbits D37 (descending), A117 (ascending) and D110 (descending) from January to April, between 2019 to 2022. ICESat-2 reference ground tracks (RGT). ICESat-2 data was collected from January to April, between 2019 to 2021, with additional ICESat-2 data from 2022 used for validation alongside snow depth measurements from weather stations.

2 Data and Methods

2.1 Sentinel-1 ΔCR as a proxy for snow depth

The Sentinel-1 mission is a two-satellite constellation, which was launched in 2014 (Sentinel-1A) and 2016 (Sentinel-1B) respectively. The satellites carry a C-band SAR instrument, providing imagery of the earth's surface in all weather conditions at approximately 20-meter resolution with a 6-day repeat-pass period (12-day repeat since the failure of Sentinel-1B in December 2021). The Sentinel-1 radar system transmits waves of a single polarization (horizontal or vertical) but receives both polarizations. Over most land areas, Sentinel-1 transmits vertically polarized waves, yielding co-polarized (VV) and cross-polarized (VH) images.

Sentinel-1 records backscatter with information about surface properties and cannot measure snow depth directly, but snow depth retrieval algorithms (Lievens et al., 2019, 2022) have been developed based on backscatter change detection. The algorithms attempt to capture changes in volume scattering within a dry snowpack, by assuming that the cross-polarized VH signal is more sensitive to volume scattering from the dry snowpack, relative to the VV signal, and that all other changes in backscatter, such as influence from soil moisture, temperature and liquid content, are mostly similar in both polarization channels (Lievens et al., 2019).

https://doi.org/10.5194/egusphere-2024-3850
Preprint. Discussion started: 17 January 2025

The increase in volume scattering is linked to snow depth by assuming that greater volume scattering between snowpack layers is more likely in deeper snowpacks. Consequently, changes in snow depth can be inferred from variations in volume scattering (Lievens et al., 2019).

Like Lievens et al., (2019), we derive ΔCR from the Sentinel-1 Ground-Range Detected (GRD) Interferometric Wide Swath (IW) dataset in Google Earth Engine (Filipponi, 2019). Prior to analysis, the Sentinel-1 scenes have gone through a pre-processing routine including thermal noise removal, radiometric calibration and range-Doppler terrain correction.

We use the equation from Lievens et al., (2022) to approximate the volume scattering within a dry snowpack (equation 1):

$$CR = 2 * VH / VV \quad \textit{(Equation 1)}$$

We then calculate the change in volume scattering ΔCR, by subtracting the measured volume scattering (CR) from any given Sentinel-1 scene in the snow accumulation season with the CR from the start of snow accumulation season ($CR_{reference}$) (Figure 2) (Equation 2):

$$\Delta CR = CR - CR_{reference} \quad \textit{(Equation 2)}$$

We define $CR_{reference}$ as the average CR within the first two weeks of Sentinel-1 images following the first day of snowfall detected by the MODIS Terra Snow Cover Daily dataset (Hall and Riggs, 2021). The snow mapping procedure of MODIS uses reflectance difference measurements from the Normalized Difference Snow Index (NDSI) which allows distinguishing the reflectance of snow from most other surface features (Hall and Riggs, 2021; Parajka and Blöschl, 2008)

To minimize the influence of soil moisture changes, which affects the scattering properties of the radar waves and hence ΔCR (Feng et al., 2021), we mask out vegetated areas using the normalized difference vegetation index (NDVI). Vegetated areas are detected from a threshold of 0.3> using an annual mean NDVI image composite derived from Sentinel-2. Pixels are classified as wet snow when the backscatter drops significantly (Longepe et al., 2009; Nagler et al., 2016; Rott et al., 2010), which we define as a drop in ΔCR above 2dB, while the land cover types of forests and water are detected and removed using the 100-meter Proba-V CGLS land cover dataset (Buchhorn et al., 2020).

For the remaining low vegetation/bare rock pixels ΔCR is smoothed spatiotemporally to reduce the impact of observational noise and spurious fluctuations (Lievens et al., 2019), using a circular focal-mean kernel of two kilometers and pixels are resampled to 500 meters pixel spacing. The imagery is smoothed temporally by calculating the average ΔCR from two images (6 days or 12 days in 2022).

In the Southern Scandinavian Mountains, Sentinel-1 orbit 37 and orbit 110 descend over the area every six days at approximately 5 am local time, while orbit 117 ascends at around 5 pm local time. For the descending orbits, the daily temperature is expected to be near its lowest, providing ideal conditions for measuring the backscatter from a dry snowpack. Warmer temperatures may cause surface melt, affecting backscatter retrievals. For each year from 2019 to 2022, during the months of January to April, orbit-specific ΔCR is derived from Sentinel-1 scenes for the three orbits: D110 (descending), D37 (descending) and A117 (ascending).

https://doi.org/10.5194/egusphere-2024-3850
Preprint. Discussion started: 17 January 2025

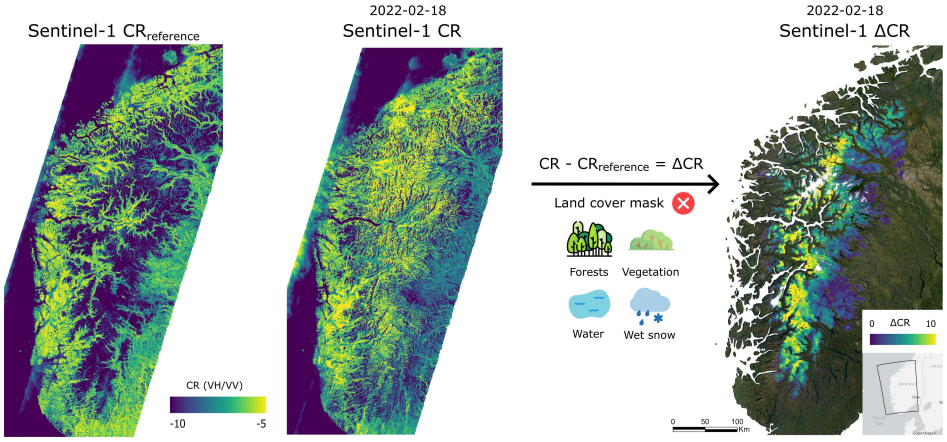

Figure 2: Sentinel-1 ΔCR. Sentinel-1 ΔCR (change in cross-polarization ratio) is derived from backscatter to be used as a proxy for snow depth. As an example, ΔCR for 2022-02-18 is derived by subtracting CR with $CR_{reference}$, where $CR_{reference}$ is the average CR of the two following Sentinel-1 images after the date snowfall is detected. Land covers where a change in CR is more likely influenced by other factors than snow accumulation are masked out using optical satellite imagery.

2.2 ICESat-2 snow depths retrieval algorithm

ICESat-2 snow depths are derived from the ATL03 geolocated photon dataset (Neumann et al., 2021) (Figure 3) using a customized surface height algorithm. The geolocated photon heights are binned along-track and a surface height is derived based on photon density (Datta and Wouters, 2021). Initially, the ICESat-2 along-track surface height is set to 10-meter spatial resolution with an along-track window width of 20 meters. ICESat-2 surface height is converted to snow depth by sampling and subtracting the height from the snow-off reference digital elevation model (DEM). We use the 10-meter Norwegian national DEM as reference height. The DEM is made up of several projects that are established individually as either point clouds based on aerial LiDAR scanning or aerial photos that have been processed through image matching (Geonorge, 2024). Slopes below 1 degree are masked out to remove water bodies and slopes above 10 degrees are masked, while ICESat-2 observations over dynamic land-cover types (forests, water bodies and glaciers) are also removed, as we expect changes in CR to be more heavily affected by factors other than snow accumulation in these regions.

The snow depths are smoothed along-track with a focal-mean filter over two kilometers and rescaled to 500-meter spatial resolution to match the Sentinel-1 ΔCR measurements. While ICESat-2 can provide accurate measurements at much higher spatial resolution (Besso et al., 2024; Deschamps-Berger et al., 2023) we trade spatial accuracy for vertical accuracy by averaging out measurement noise related to ICESat-2's 13-meter footprint and local height difference errors between ICESat-2 and our reference DEM.

These spatial resolution parameters were set based on a sensitivity analysis comparing the ICESat-2 surface heights with the Norwegian DEM and ArcticDEM (Morin et al., 2016) in snow-free conditions (S1). The sensitivity analysis in snow-off conditions was conducted to estimate the accuracy in snow-on conditions and

https://doi.org/10.5194/egusphere-2024-3850
Preprint. Discussion started: 17 January 2025

revealed a standard deviation between ICESat-2 surface height and the Norwegian DEM of 0.52 meters and a bias of -0.11 meters (S1). ICESat-2 surface heights are also compared to the 10-meter ArcticDEM mosaic, which covers the whole arctic region. Here we observed a standard deviation of 1.01 meters and a bias of -0.53 meters (S1).

The ICESat-2 snow depth retrieval algorithm is used on 30 ICESat-2 tracks from January to April for the years 2019-2021, retrieving 21309 snow depths point measurements spread across the Southern Norwegian Mountains (Figure 3).

https://doi.org/10.5194/egusphere-2024-3850
Preprint. Discussion started: 17 January 2025

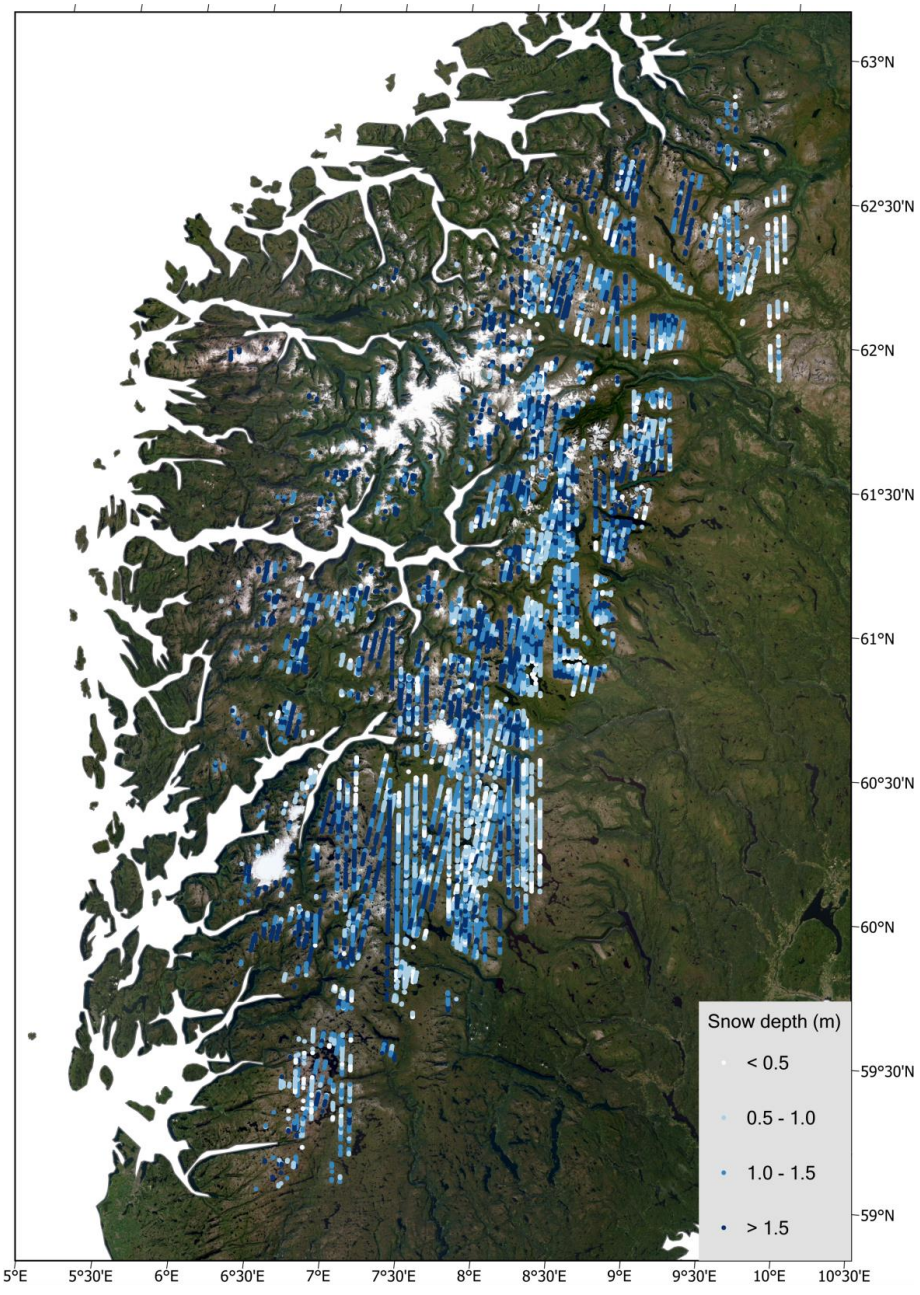

Figure 3: ICESat-2 snow depths. 21309 ICESat-2 snow depths derived between January-April, 2019-2021. Geolocated photons in the ATL03 dataset are converted into ICESat-2 surface heights, and a snow depth is calculated based on the difference in height between our ICESat-2 snow-on surface heights and the snow-off reference DEM. The snow depths are smoothed over two kilometers using a focal-mean filter and resampled to 500 meters along-track.

https://doi.org/10.5194/egusphere-2024-3850
Preprint. Discussion started: 17 January 2025

2.3 Linear regression

To estimate snow depths from Sentinel-1, we compare our stack of Sentinel-1 ΔCR images to the temporally nearest ICESat-2 track (Figure 4a). For each average ICESat-2 snow depth measured at 500-meter intervals along-track, we extract the smoothed and resampled 500-meter value of ΔCR. To capture the spatiotemporal relationship between Sentinel-1 ΔCR and snow depth, we retrieve ΔCR from the 21309 ICESat-2 snow depths derived from the 30 ICESat-2 tracks between January – April, 2019-2021.

Through ordinary least squared linear regression (OLS), we estimate Sentinel-1 snow depths based on the fit between ΔCR and snow depth. Sentinel-1 descending orbits D110 (Figure 4b) and D37 returns similar linear relationships with snow depth, with a slope of 0.21/0.23 meters/dB and intercept of 0.68/0.65 meters, whereas the slope and intercept are 0.15 meters/dB and 0.98 meters for the ascending orbit A117 (Figure S2). The Pearson correlation coefficient (Pearson-R) is used to measure the strength and direction of the linear correlation between ΔCR and ICESat-2 snow depth. We choose only to compute Sentinel-1 derived snow depths from the descending orbits, as they showed a stronger correlation than the ascending orbit. The Pearson-R is 0.56/0.62 for the descending orbits and 0.36 for the ascending orbit (Figure S3).

https://doi.org/10.5194/egusphere-2024-3850
Preprint. Discussion started: 17 January 2025

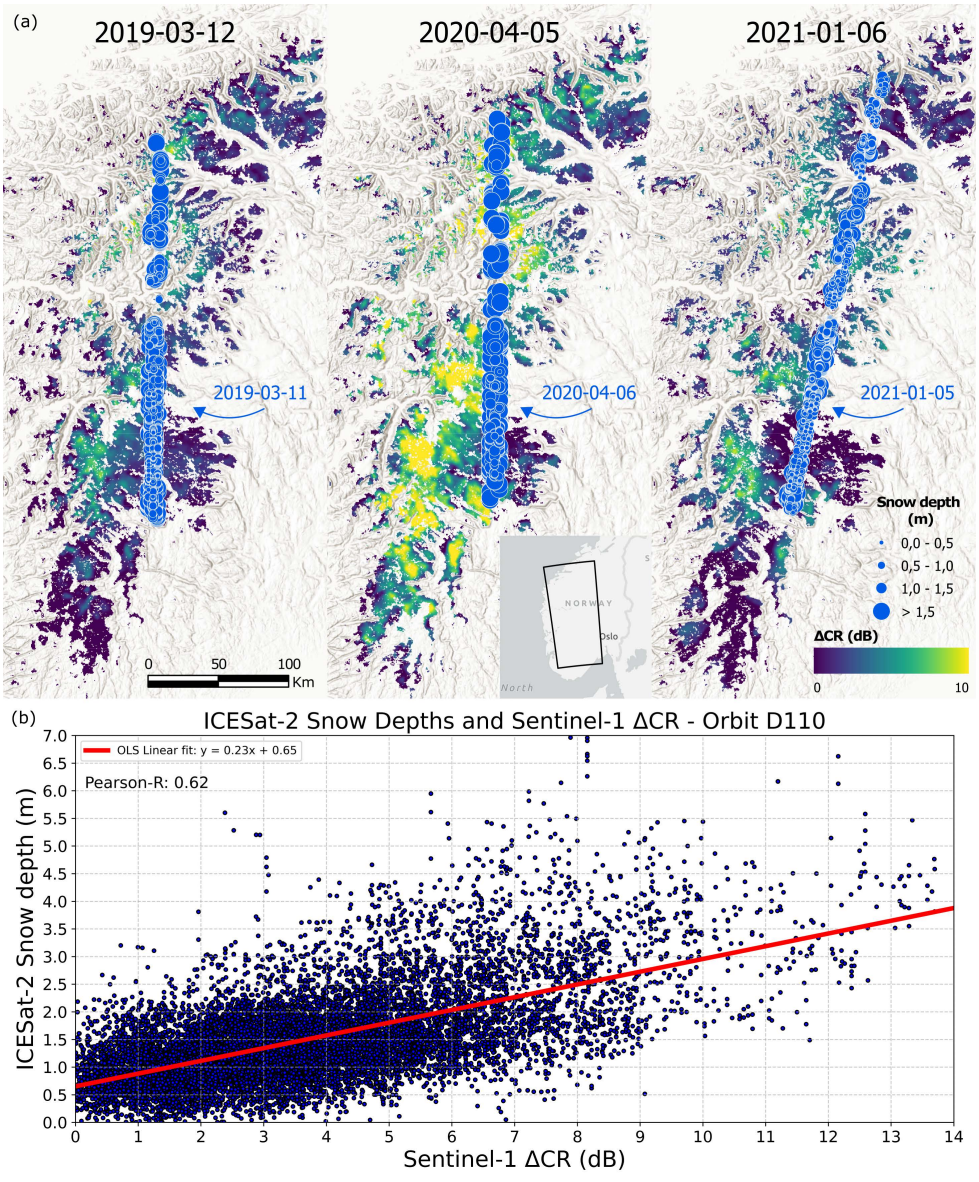

Figure 4: Multitemporal sampling and OLS linear regression. (a) Illustrates location and date of three ICESat-2 tracks (blue dots), and how they are matched with the temporally nearest imagery of Sentinel-1 ΔCR. **(b)** Relationship between ICESat-2 snow depths and Sentinel-1 ΔCR for orbit D110. Ordinary Least Squares (OLS) is used to fit and retrieve Sentinel-1 snow depths.

https://doi.org/10.5194/egusphere-2024-3850
Preprint. Discussion started: 17 January 2025

2.4 Validation data

We evaluate our snow depth estimates against point-scale snow depth observations from 12 weather stations from the Norwegian Meteorological Institute (MET) and the snow model seNorge from the Norwegian Water Resources and Energy Directorate between January and April, 2019-2022. The seNorge model provides snow depths in a 1km^2 grid based on precipitation and air temperature data from the national observation network of MET weather stations (Saloranta, 2016). Before modelling snow depths, the input data is interpolated into a nationwide grid of 1 km cells which are height-corrected using a DTM (Saloranta, 2016). A temperature threshold determines whether precipitation is classified as snow or rain. If the temperature is below 0.5° C, the model assumes that the precipitation comes as snow, while anything above this temperature is interpreted as rain (NVE, 2024). Temperature also determines whether or not the model predicts snowmelt, using a threshold value of 0° C (NVE, 2024).

Results are also compared with two ICESat-2 tracks from January and March 2022 in the high mountains of western Hardangervidda, to investigate the accuracy in one of the most remote regions of our study area. Lastly, we investigate local snow depth variability through 279 snow depth measurements obtained during a field excursion to the Hardangervidda plateau from February 21 to 25, 2022 in the three regions, Dyranut, Røldalsfjellet and Haukeliseter. Snow depths were measured using an avalanche probe every ~10 m in a cross-formation. We chose this interval and formation to be able to capture local variations in landscape aspect in multiple directions. Using the Android app SW Maps to record the location of each observation, we detected a horizontal positional accuracy of up to 5 m.

3 Results and discussion

In the Southern Norwegian Mountains, precipitation is dominated by frontal storm events most of the year with inland regions also influenced by convective precipitation (Rizzi et al., 2017). Increased precipitation is found in the westeren coastal mountains, as this mountain range works as a significant orographic feature for the dominant westerly winds (Skaugen and Melvold, 2019). Precipitation falls as snow in the high mountains from around mid-September, reaching maximum snow depth in mid to late April (Skaugen and Melvold, 2019).

Figure 5a-b shows how our Sentinel-1 ΔCR captures the accumulation of snow between January and April 2022, where a strong increase in snow depth can be observed in the westeren part of the mountain range. In the same region, a strong decrease in ΔCR is observed and flagged as wet snow starting in March 2022 (Figure 5b). Similar spatial snow depth distributions are observed on a large scale across our study region, with the deepest snow observed in the years of 2020 and 2022 (Figure 5c).

https://doi.org/10.5194/egusphere-2024-3850
Preprint. Discussion started: 17 January 2025

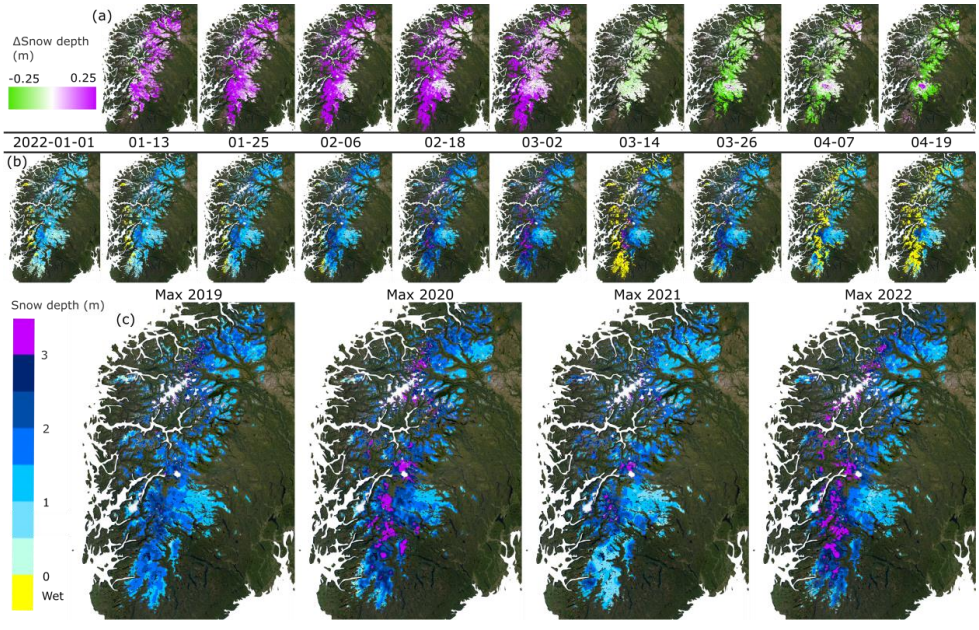

Figure 5: Sentinel-1 snow depth time-series in 2022 and maximum snow depth. **(a)** Change in snow depth compared to previous Sentinel-1 scene and **(b)** total snow depth derived from Sentinel-1 orbit D110, January through April 2022. A strong accumulation of snow can be observed in the western parts of the southeren Norwegian mountains from January until mid-March, where snow melt is detected. **(c)** Maximum Sentinel-1 derived snow depth for 2019-2022.

3.1 Regional comparison with snow model

Maximum composites of snow depths from Sentinel-1 (Figure 6a) and the SeNorge snow model for 2022 reveal a large discrepancy of several meters along the western coastal mountains (Figure 6b-c). Studies evaluating the SeNorge model found that the model is overestimating snow depth in the Southern Norwegian Mountains by 50-54%, while overestimating SWE in the range of 86-100 %, increasing with elevation (Saloranta, 2012). While our Sentinel-1 maximum composite from 2022 reaches depths of up to 4 meters, SeNorge predicts 7-8 meters of snow depth.

https://doi.org/10.5194/egusphere-2024-3850
Preprint. Discussion started: 17 January 2025

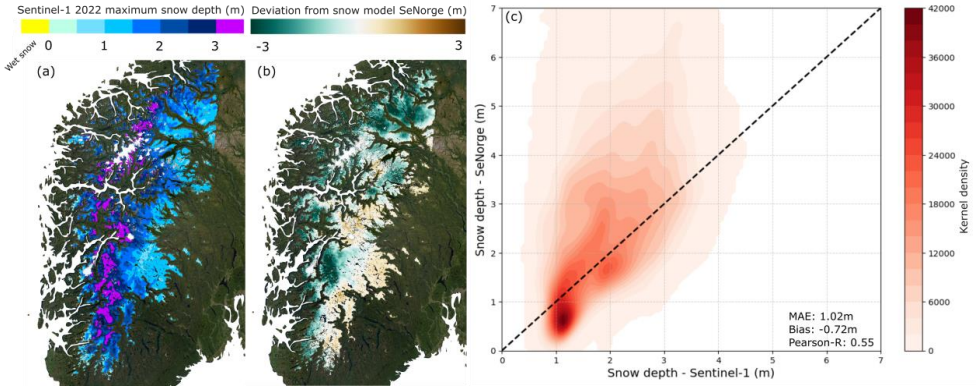

Figure 6: Sentinel-1 maximum snow depth of 2022 compared to SeNorge snow model in 2022. **(a)** Comparison of maximum snow depth in 2022 using Sentinel-1 and SeNorge snow model. **(b)** Spatial distribution of Sentinel-1 snows depth **(c)** Spatial deviation of maximum snow depth between Sentinel-1 and SeNorge snow model.

3.2 Subregional comparison with ICESat-2

The largest discrepancies between Sentinel-1 and SeNorge are found in the remote mountainous regions, furthest from the weather stations (Figure 1c and Figure 6c). To evaluate the performance in these regions we compared it with two ICESat-2 tracks covering the western part of the Hardangervidda plateau at two timestamps, 6. January and 9. March 2022 (Figure 7). Though ICESat-2 snow depths should not be considered as ground truth (Figure S1) and will be positively biased towards our ICESat-2 calibrated Sentinel-1 snow depths, we observe a similar pattern to previous studies (Melvold and Skaugen, 2013; Saloranta, 2012), as SeNorge overpredicts snow depths with 89% (Bias = 155 cm), while Sentinel-1 only overestimates by 12% (Bias = 21 cm).

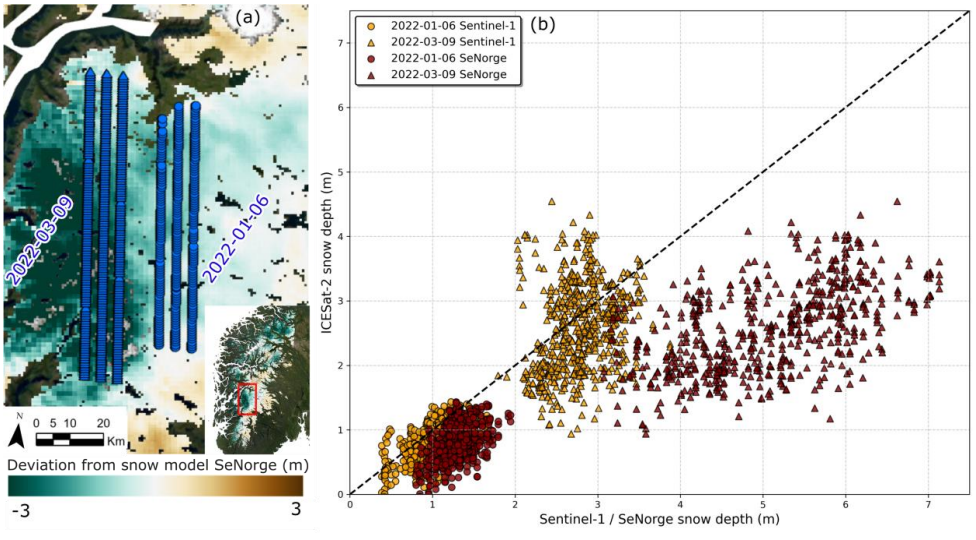

https://doi.org/10.5194/egusphere-2024-3850
Preprint. Discussion started: 17 January 2025

Figure 7: Comparing Sentinel-1 derived snow depths with ICESat-2 tracks over western Hardangervidda. **(a)** Coverage of two ICESat-2 tracks from 2022 over western Hardangervidda mountains, where strong deviations between the SeNorge snow model Sentinel-1 are observed. **(b)** Plot of Sentinel-1 and SeNorge predicted snow depths compared to the two ICESat-2 tracks.

3.3 Local comparison to weather stations and in-situ measurements

Local scale snow depth measurements obtained by weather stations and in-situ measurements were compared against Sentinel-1 and SeNorge. The mean absolute error (MAE) consistently ranging at approximately 60 cm between Sentinel-1, weather stations and SeNorge with no clear patterns across the four years (Table 1). The SeNorge snow model consistently overpredicts snow depths compared to the weather stations, with an average bias of 52 cm between January and April, 2019-2022, whereas Sentinel-1 has a lower average bias of 19 cm. SeNorge has a much stronger linear relationship with the weather stations, presumably because the model uses the weather station data as input, with an average Pearson-R coefficient of 0.83 and p-values ranging between 0-0.13 compared to an average Pearson-R of 0.33 and p-value between 0.15-0.48 for Sentinel-1. Sentinel-1 performs slightly better in 2020 (Pearson-R of 0.39) and 2022 (Pearson-R of 0.53), where deeper snow is present on average across the weather stations. The accuracy of Sentinel-1 varies significantly between each weather station (Figure S4). One source of error is that we are comparing snow depths averaged over two kilometers with a snow depth point-measurement, which is heavily influenced by the weather stations topographic position in the landscape. On the Hardangervidda plateau, snow depths can vary between 0 and 10 meters on hillslope scale, but this variability is either strongly reduced or not captured when the averaging area increases to one kilometer (Melvold and Skaugen, 2013).

https://doi.org/10.5194/egusphere-2024-3850
Preprint. Discussion started: 17 January 2025

Table 1: Comparing Sentinel-1 derived snow depths with weather station measurements. Local scale validation against twelve weather stations across the Southern Norwegian mountains. At each location, the weather stations snow depth measurements Sentinel-1 and SeNorge are compared. The values are based on the average MAE, bias, Pearson-R coefficient and p-value derived at each weather station, aggregated per year in the months of January through April, for the years 2019-2022.

		2019	2020	2021	2022
Average snow depth across stations (cm)		*88*	*170*	*90*	*140*
Sentinel-1 compared to weather stations	MAE	*78*	*67*	*62*	*70*
	Bias	*31*	*-5*	*32*	*18*
	Pearson-R	*0.21*	*0.39*	*0.19*	*0.53*
	P-value	*0.48*	*0.15*	*0.47*	*0.16*
Sentinel-1 compared to SeNorge snow model	MAE	*40*	*78*	*76*	*69*
	Bias	*2*	*-43*	*-42*	*-40*
	Pearson-R	*0.13*	*0.49*	*0.27*	*0.68*
	P-value	*0.21*	*0.08*	*0.37*	*0.06*
SeNorge snow model compared to weather stations	MAE	*61*	*58*	*70*	*76*
	Bias	*40*	*38*	*69*	*61*
	Pearson-R	*0.83*	*0.87*	*0.82*	*0.81*
	P-value	*0.13*	*0.09*	*0*	*0.01*

We studied local snow depth variability through our 279 snow depth measurements obtained during the field excursion around the Hardangervidda plateau (Figure 8a). At six sites, the mean in-situ snow depth was compared to the snow depth from Sentinel-1 and the SeNorge snow model (Figure 8b). Sentinel-1 has a MAE of 47 cm with a Bias of -18 cm, while SeNorge has a MAE of 100 cm and bias of 100 cm. While our in-situ measurements are only recorded at one point in time, we can observe the same trend of SeNorge overpredictions as documented (Melvold and Skaugen, 2013; Saloranta, 2012) and observed on local and subregional scales. Our Sentinel-1 snow depth seems to more accurately predict the magnitude of snowfall at these sites, however large deviations can still be observed, as Sentinel-1 predicts around 140 cm of snow depth at both sites, D3 and H1, while the average site snow depth is 95 cm for D3 and 226 cm for H1 (Figure 8b).

In 2022, Røldalsfjellet had a large accumulation of snow from mid-January to early March, captured at various spatial resolutions by the weather station, Sentinel-1 and SeNorge (Figure 8c). On 2022-02-23, we measured 48 snow depths in Røldalsfjellet about 300 to 600 m from the local weather station (Figure 8d). The snow depths varied between 1.7 meters and four meters, with up to 1.5 meters difference in snow depth between measurements ten meters apart. The average snow depth was 257 cm with a standard deviation of 57 cm. The different datasets disagree about the magnitude of snow accumulation, with the weather station recording a snow depth of 205 cm, while SeNorge predicted 340 cm snow depth, and the nearest Sentinel-1 derived snow depth was 312 cm.

https://doi.org/10.5194/egusphere-2024-3850
Preprint. Discussion started: 17 January 2025

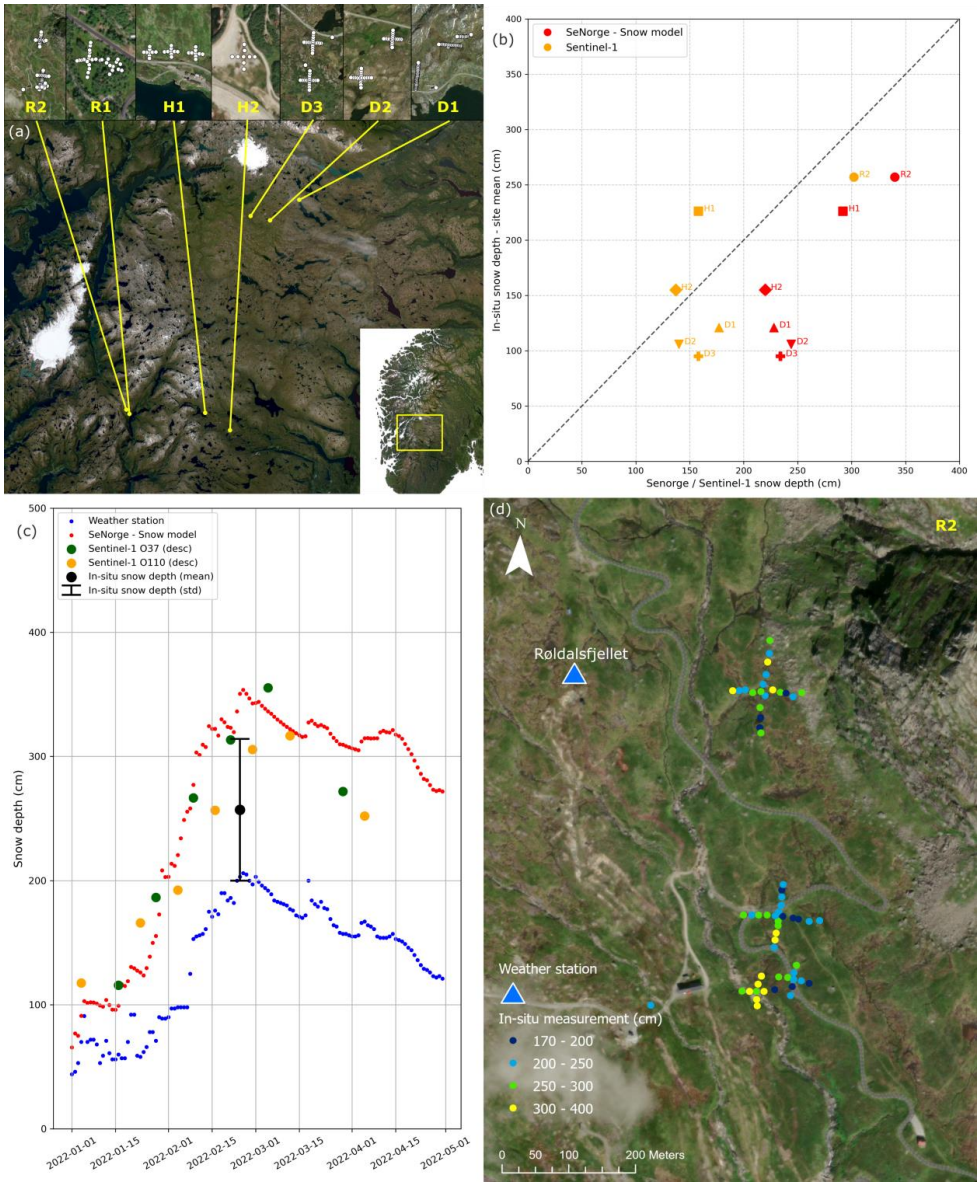

Figure 8: In-situ measurements around Hardangervidda. **(a)** Locations of the in-situ measurement sites around Hardangervidda. Measurements were recorded from February 21 to 25, 2022 in the three regions, Dyranut, Røldalsfjellet and Haukeliseter. **(b)** Mean snow depth at in-situ measurement sites compared to Sentinel-1 (orange) and the SeNorge snow model (red). **(c-d)** At site Røldalsfjellet-2 (R2), in-situ snow depth measurements are compared to the nearby weather station, Sentinel-1 and SeNorge.

https://doi.org/10.5194/egusphere-2024-3850
Preprint. Discussion started: 17 January 2025

3.4 Sentinel-1 snow depths

The Sentinel-1 ΔCR measure captures changes in volume scattering, which correlate with snow depth (i.e., a deeper snow layer causes a higher proportion of volume scattering). However, ΔCR is also influenced by density, microstructures within the snowpack, and freeze-thaw events (Bernier and Fortin, 1998; Brangers et al., 2024; Lievens et al., 2022), which complicates the retrieval of snow depth. Furthermore C-band backscatters may also be influenced by temperature, soil moisture, and wet snow. (Bergstedt et al., 2018; Feng et al., 2021; Shi and Dozier, 2000). Dunmire et al., (2024) found a statistically significant relationship between CR and snow depths between 1-3 m, while Hoppinen et al., (2024) reported poor performance between Sentinel-1 and snow depths from airborne lidar surveys, with moderate improvements for snow depths exceeding 1.5 m.

Our calibration with ICESat-2 observations revealed that Sentinel-1 can observe changes in ΔCR when snow depth exceeds 60 cm (for descending orbit 110) (Figure 4b). Similarly, Sentinel-1 had the best performance in the years when the average snow depth exceeded 1 meter across weather stations (Pearson-R = 0.39-0.68) with an MAE of approximately 70 cm, similar to the SeNorge snow model. Furthermore, our subregional comparison with ICESat-2 revealed that Sentinel-1 outperforms the SeNorge snow model's ability to accurately estimate magnitude of snowfall (S1 bias = 21 cm; SeNorge bias = 100 cm), but that limitation persists in Sentinel-1's ability to capture the snow variability (MAE = 44 cm) (Figure 7). The same pattern was observed when evaluated against the six sites of in-situ snow depth measurements (Figure 8).

With Sentinel-1, we can estimate the magnitude of snow depths more accurately in remote regions, because our estimates are calibrated with ICESat-2 observations that cover these areas. On the contrary, the overestimation of snow depths from the SeNorge snow model (Melvold and Skaugen, 2013; Saloranta, 2012) is expected, as the models input is sparse ground observations. The large discrepancies of several meters in some regions between our snow depth estimates and SeNorge (Figure 6) reveal a knowledge gap that is hard to capture if you only have sparse ground observations. It further explains how calibration and validation of Sentinel-1 snow depths can be bias if either or both modelled and weather station data is used in the calibration and evaluation phases, and might explain why Sentinel-1 derived snow depths have performed worse when evaluated with photogrammetric surveys (Dunmire et al., 2024) and airborne LiDAR (Hoppinen et al., 2024).

ICESat-2 offers an improved way to estimate the relationship between an increase in ΔCR and snow depth. Instead of relying on data from weather stations, modelled data or surveys, the correlation is based on thousands of multitemporal snow depth measurements captured by ICESat-2 in remote regions where little to no prior information about snow depth has been measured before, therefore offering a more robust and less biased opportunity to calibrate Sentinel-1 derived snow depths. Future endeavors could expand this methodology to other regions. Since ICESat-2 has global coverage, the current limitation is the availability of a suitable reference DEM. In polar regions ICESat-2 has repeat track coverage, removing the need for reference DEMs. The expansion of this research into other remote regions, where in-situ measurements are few and far between, would further contextualize its large-scale, operational applicability.

https://doi.org/10.5194/egusphere-2024-3850
Preprint. Discussion started: 17 January 2025

4 Conclusion

In this study, we developed a satellite-based algorithm to derive timely estimates of snow depths in deep dry snow at 500-meter spatial resolution using Sentinel-1 volume scattering and ICESat-2. Specifically, we found that Sentinel-1 ΔCR can capture snow depth changes in dry snow above 0.6 meters with an MAE of 0.5-0.7 meters and moderate correlations for descending orbits (Pearson-R: 0.56/0.62) over the Southern Norwegian Mountains.

Our ICESat-2 calibrated Sentinel-1 snow depths demonstrates improved accuracy in predicting snow depth compared to the SeNorge snow model, by relying on thousands of ICESat-2 observations, which serves as a robust calibration dataset to estimate the relationship between an increase in Sentinel-1 volume scattering and snow depth. Across in-situ sites, our estimates achieved an MAE of 47 cm and a bias of -18 cm, while SeNorge showed larger errors (MAE and Bias = 100 cm). Compared to ICESat-2, we achieved an MAE of 44 cm and a bias of 21 cm, whereas SeNorge exhibited significant overestimation (MAE and Bias = 155 cm). In some remote regions, discrepancies of several meters were observed between Sentinel-1 and the SeNorge snow model, emphasizing the value of ICESat-2 observations in improving snow depth estimation.

While Sentinel-1 has inherent limitations, this methodology could be integrated to improve snow model accuracy in remote regions that experience heavy snowfall. Timely snow depth estimates are critical for hydropower management in Norway and for monitoring changes in seasonal snowfall under a changing climate. This study demonstrates how ICESat-2 observations enhance the accuracy and utility of Sentinel-1-derived snow depths, improving snow monitoring in data-sparse regions with potential global applications.

Data availability

The ICESat-2 calibrated Sentinel-1 snow depth estimates will be available for download online upon acceptance of the manuscript (DOI INSERT).

ICESat-2 ATL03 data can be downloaded from NSIDC: https://nsidc.org/data/atl03/versions/5

Sentinel-1 GRD dataset and auxiliary datasets can be accessed through Google Earth Engine: https://developers.google.com/earth-engine/datasets

In-situ snow depth measurements will be available upon acceptance (DOI INSERT)

Author contributions

RM wrote the main manuscript and led the data analysis. RM, MPS, MLR and AAB designed the study and wrote the initial draft. RM and MPS conducted fieldwork and data collection. MD, JKA and AAB provided extensive guidance in analysis and editing of the manuscript.

Competing Interests

The authors declare that they have no conflict of interest.

References

Adam, J. C., Hamlet, A. F., and Lettenmaier, D. P.: Implications of global climate change for snowmelt hydrology in the twenty-first century, Hydrological Processes, 23, 962–972, https://doi.org/10.1002/hyp.7201, 2009.

https://doi.org/10.5194/egusphere-2024-3850
Preprint. Discussion started: 17 January 2025

Bergstedt, H., Zwieback, S., Bartsch, A., and Leibman, M.: Dependence of C-Band Backscatter on Ground Temperature, Air Temperature and Snow Depth in Arctic Permafrost Regions, Remote Sensing, 10, 142, https://doi.org/10.3390/rs10010142, 2018.

Bernier, M. and Fortin, J.-P.: The potential of times series of C-Band SAR data to monitor dry and shallow snow cover, IEEE Trans. Geosci. Remote Sensing, 36, 226–243, https://doi.org/10.1109/36.655332, 1998.

Besso, H., Shean, D., and Lundquist, J. D.: Mountain snow depth retrievals from customized processing of ICESat-2 satellite laser altimetry, Remote Sensing of Environment, 300, 113843, https://doi.org/10.1016/j.rse.2023.113843, 2024.

Bormann, K. J., Brown, R. D., Derksen, C., and Painter, T. H.: Estimating snow-cover trends from space, Nature Clim Change, 8, 924–928, https://doi.org/10.1038/s41558-018-0318-3, 2018.

Brangers, I., Marshall, H.-P., De Lannoy, G., Dunmire, D., Mätzler, C., and Lievens, H.: Tower-based C-band radar measurements of an alpine snowpack, The Cryosphere, 18, 3177–3193, https://doi.org/10.5194/tc-18-3177-2024, 2024.

Buchhorn, M., Lesiv, M., Tsendbazar, N.-E., Herold, M., Bertels, L., and Smets, B.: Copernicus Global Land Cover Layers—Collection 2, Remote Sensing, 12, 1044, https://doi.org/10.3390/rs12061044, 2020.

Datta, R. T. and Wouters, B.: Supraglacial lake bathymetry automatically derived from ICESat-2 constraining lake depth estimates from multi-source satellite imagery, The Cryosphere, 15, 5115–5132, https://doi.org/10.5194/tc-15-5115-2021, 2021.

Deems, J. S., Painter, T. H., and Finnegan, D. C.: Lidar measurement of snow depth: a review, Journal of Glaciology, 59, 467–479, https://doi.org/10.3189/2013JoG12J154, 2013.

Deschamps-Berger, C., Gascoin, S., Shean, D., Besso, H., Guiot, A., and López-Moreno, J. I.: Evaluation of snow depth retrievals from ICESat-2 using airborne laser-scanning data, The Cryosphere, 17, 2779–2792, https://doi.org/10.5194/tc-17-2779-2023, 2023.

Du, J., Shi, J., and Rott, H.: Comparison between a multi-scattering and multi-layer snow scattering model and its parameterized snow backscattering model, Remote Sensing of Environment, 114, 1089–1098, https://doi.org/10.1016/j.rse.2009.12.020, 2010.

Dunmire, D., Lievens, H., Boeykens, L., and De Lannoy, G. J. M.: A machine learning approach for estimating snow depth across the European Alps from Sentinel-1 imagery, Remote Sensing of Environment, 314, 114369, https://doi.org/10.1016/j.rse.2024.114369, 2024.

Feng, T., Hao, X., Wang, J., Li, H., and Zhang, J.: Quantitative Evaluation of the Soil Signal Effect on the Correlation between Sentinel-1 Cross Ratio and Snow Depth, Remote Sensing, 13, 4691, https://doi.org/10.3390/rs13224691, 2021.

Filipponi, F.: Sentinel-1 GRD Preprocessing Workflow, in: 3rd International Electronic Conference on Remote Sensing, International Electronic Conference on Remote Sensing, 11, https://doi.org/10.3390/ECRS-3-06201, 2019.

Geonorge: Høydedata, 2024.

Hall, D. K. and Riggs, G. A.: MODIS/Aqua Snow Cover Daily L3 Global 500m Grid, Version 61, https://doi.org/10.5067/MODIS/MYD10A1.061, 2021.

Harder, P., Schirmer, M., Pomeroy, J., and Helgason, W.: Accuracy of snow depth estimation in mountain and prairie environments by an unmanned aerial vehicle, The Cryosphere, 10, 2559–2571, https://doi.org/10.5194/tc-10-2559-2016, 2016.

https://doi.org/10.5194/egusphere-2024-3850
Preprint. Discussion started: 17 January 2025

Hoppinen, Z., Palomaki, R. T., Brencher, G., Dunmire, D., Gagliano, E., Marziliano, A., Tarricone, J., and Marshall, H.-P.: Evaluating snow depth retrievals from Sentinel-1 volume scattering over NASA SnowEx sites, The Cryosphere, 18, 5407–5430, https://doi.org/10.5194/tc-18-5407-2024, 2024.

Kendra, J. R., Sarabandi, K., and Ulaby, F. T.: Radar measurements of snow: experiment and analysis, IEEE Transactions on Geoscience and Remote Sensing, 36, 864–879, https://doi.org/10.1109/36.673679, 1998.

King, J., Kelly, R., Kasurak, A., Duguay, C., Gunn, G., Rutter, N., Watts, T., and Derksen, C.: Spatio-temporal influence of tundra snow properties on Ku-band (17.2 GHz) backscatter, Journal of Glaciology, 61, 267–279, https://doi.org/10.3189/2015JoG14J020, 2015.

Kongoli, C., Key, J., and Smith, T. M.: Mapping of Snow Depth by Blending Satellite and In-Situ Data Using Two-Dimensional Optimal Interpolation—Application to AMSR2, Remote Sensing, 11, 3049, https://doi.org/10.3390/rs11243049, 2019.

Lievens, H., Demuzere, M., Marshall, H.-P., Reichle, R. H., Brucker, L., Brangers, I., de Rosnay, P., Dumont, M., Girotto, M., Immerzeel, W. W., Jonas, T., Kim, E. J., Koch, I., Marty, C., Saloranta, T., Schöber, J., and De Lannoy, G. J. M.: Snow depth variability in the Northern Hemisphere mountains observed from space, Nat Commun, 10, 4629, https://doi.org/10.1038/s41467-019-12566-y, 2019.

Lievens, H., Brangers, I., Marshall, H.-P., Jonas, T., Olefs, M., and De Lannoy, G.: Sentinel-1 snow depth retrieval at sub-kilometer resolution over the European Alps, The Cryosphere, 16, 159–177, https://doi.org/10.5194/tc-16-159-2022, 2022.

Longepe, N., Allain, S., Ferro-Famil, L., Pottier, E., and Durand, Y.: Snowpack Characterization in Mountainous Regions Using C-Band SAR Data and a Meteorological Model, IEEE Transactions on Geoscience and Remote Sensing, 47, 406–418, https://doi.org/10.1109/TGRS.2008.2006048, 2009.

López-Moreno, J. I., Fassnacht, S. R., Heath, J. T., Musselman, K. N., Revuelto, J., Latron, J., Morán-Tejeda, E., and Jonas, T.: Small scale spatial variability of snow density and depth over complex alpine terrain: Implications for estimating snow water equivalent, Advances in Water Resources, 55, 40–52, https://doi.org/10.1016/j.advwatres.2012.08.010, 2013.

Magnusson, J., Nævdal, G., Matt, F., Burkhart, J. F., and Winstral, A.: Improving hydropower inflow forecasts by assimilating snow data, Hydrology Research, 51, 226–237, https://doi.org/10.2166/nh.2020.025, 2020.

Melvold, K. and Skaugen, T.: Multiscale spatial variability of lidar-derived and modeled snow depth on Hardangervidda, Norway, Annals of Glaciology, 54, 273–281, https://doi.org/10.3189/2013AoG62A161, 2013.

Meteorologisk Institutt: https://www.met.no/en, last access: 29 November 2024.

Morin, P., Porter, C., Cloutier, M., Howat, I., Noh, M.-J., Willis, M., Bates, B., Willamson, C., and Peterman, K.: ArcticDEM; A Publically Available, High Resolution Elevation Model of the Arctic, EPSC2016-8396, 2016.

Nagler, T., Rott, H., Ripper, E., Bippus, G., and Hetzenecker, M.: Advancements for Snowmelt Monitoring by Means of Sentinel-1 SAR, Remote Sensing, 8, 348, https://doi.org/10.3390/rs8040348, 2016.

Neumann, T. A., A. Brenner, D. Hancock, J. Robbins, J. Saba, K. Harbeck, A. Gibbons, J. Lee, S. B. Luthcke, and T. Rebold: ATLAS/ICESat-2 L2A Global Geolocated Photon Data, version 5, https://doi.org/10.5067/ATLAS/ATL03.005, 2021.

Nolan, M., Larsen, C., and Sturm, M.: Mapping snow depth from manned aircraft on landscape scales at centimeter resolution using structure-from-motion photogrammetry, The Cryosphere, 9, 1445–1463, https://doi.org/10.5194/tc-9-1445-2015, 2015.

NVE: SeNorge - Snow maps and climate maps in Norway, 2024.

https://doi.org/10.5194/egusphere-2024-3850
Preprint. Discussion started: 17 January 2025

Parajka, J. and Blöschl, G.: Spatio-temporal combination of MODIS images – potential for snow cover mapping, Water Resources Research, 44, https://doi.org/10.1029/2007WR006204, 2008.

Pivot, F. C.: C-Band SAR Imagery for Snow-Cover Monitoring at Treeline, Churchill, Manitoba, Canada, Remote Sensing, 4, 2133–2155, https://doi.org/10.3390/rs4072133, 2012.

Qin, Y., Abatzoglou, J. T., Siebert, S., Huning, L. S., AghaKouchak, A., Mankin, J. S., Hong, C., Tong, D., Davis, S. J., and Mueller, N. D.: Agricultural risks from changing snowmelt, Nat. Clim. Chang., 10, 459–465, https://doi.org/10.1038/s41558-020-0746-8, 2020.

Rizzi, J., Nilsen, I. B., Stagge, J. H., Gisnås, K., and Tallaksen, L. M.: Five decades of warming: impacts on snow cover in Norway, Hydrology Research, 49, 670–688, https://doi.org/10.2166/nh.2017.051, 2017.

Rott, H., Yueh, S. H., Cline, D. W., Duguay, C., Essery, R., Haas, C., Hélière, F., Kern, M., Macelloni, G., Malnes, E., Nagler, T., Pulliainen, J., Rebhan, H., and Thompson, A.: Cold Regions Hydrology High-Resolution Observatory for Snow and Cold Land Processes, Proceedings of the IEEE, 98, 752–765, https://doi.org/10.1109/JPROC.2009.2038947, 2010.

Saloranta, T. M.: Simulating snow maps for Norway: description and statistical evaluation of the seNorge snow model, The Cryosphere, 6, 1323–1337, https://doi.org/10.5194/tc-6-1323-2012, 2012.

Saloranta, T. M.: Operational snow mapping with simplified data assimilation using the seNorge snow model, Journal of Hydrology, 538, 314–325, https://doi.org/10.1016/j.jhydrol.2016.03.061, 2016.

Shi, J. and Dozier, J.: Estimation of snow water equivalence using SIR-C/X-SAR. II. Inferring snow depth and particle size, IEEE Transactions on Geoscience and Remote Sensing, 38, 2475–2488, https://doi.org/10.1109/36.885196, 2000.

Skaugen, T. and Melvold, K.: Modeling the Snow Depth Variability With a High-Resolution Lidar Data Set and Nonlinear Terrain Dependency, Water Resources Research, 55, 9689–9704, https://doi.org/10.1029/2019WR025030, 2019.

Treichler, D. and Kääb, A.: Snow depth from ICESat laser altimetry — A test study in southern Norway, Remote Sensing of Environment, 191, 389–401, https://doi.org/10.1016/j.rse.2017.01.022, 2017.

Ulaby, F. T., Stiles, W. H., and Abdelrazik, M.: Snowcover Influence on Backscattering from Terrain, IEEE Transactions on Geoscience and Remote Sensing, GE-22, 126–133, https://doi.org/10.1109/TGRS.1984.350604, 1984.